IEEE Access
Multidisciplinary | Rapid Review | Open Access Journal

Received February 12, 2020, accepted March 5, 2020, date of publication March 13, 2020, date of current version March 24, 2020.

Digital Object Identifier 10.1109/ACCESS.2020.2980687

Control of MagLev System Using Supertwisting and Integral Backstepping Sliding Mode Algorithm

HAFIZ MIAN MUHAMMAD ADIL, SHAHZAD AHMED, AND IFTIKHAR AHMAD
School of Electrical Engineering and Computer Science, National University of Sciences and Technology (NUST), Islamabad 44000, Pakistan
Corresponding author: Iftikhar Ahmad (iftikhar.rana@seecs.edu.pk)

ABSTRACT Magnetic Levitation systems are nonlinear, frictionless and noiseless which use electromagnetic fields to hover ferromagnetic objects in air. For this purpose, we have proposed Supertwisting and Integral Backstepping sliding mode controllers. The designed controllers ensure the air gap to be maintained at the desired value while tracking the magnetic flux and momentum to their respective references. The stability analysis of the proposed controllers has been presented using Lyapunov theory which proves the global asymptotic stability of the system. The performance of the proposed controllers is analyzed using ODE 45 solver in MATLAB/Simulink environment. The proposed controllers reduce the chattering and improves the dynamic response of the system. Robustness of the proposed controllers has been checked by adding noise and disturbance in system's state space model. Furthermore, comparison of proposed controllers with each other, with conventional PI and recently published nonlinear controllers for MagLev system in terms of dynamic response has also been presented. The results show that the dynamic behavior of supertwisting sliding mode controller is best among analyzed controllers.

INDEX TERMS Magnetic levitation (MagLev), integral backstepping sliding mode controller (IBS-SMC), supertwisting sliding mode controller (ST-SMC), Lyapunov stability.

I. INTRODUCTION

The basic principle of MagLev system is to apply electric voltage to an electromagnet in order to produce a magnetic force, which serves as a lifting tool against the gravitational force, necessary for the levitation of ferromagnetic object (for instance a ball) in the air. No physical support is required and this eliminates the problem of friction losses [1], [2].

Now-a-days MagLev is becoming an eminent technology due to its contact-less property. It also has minimal maintenance cost due to no wear and tear of parts. Therefore, the life span of MagLev system is very long. It has a vast range of applications in various fields of everyday life i.e. in transportation [3]–[5], bearing-less motors [6], [7], bio-medical [8], industries [9], [10], launching of rockets [11], [12], in levitation of metals etc.

Magnetic levitation systems are highly nonlinear, therefore designing nonlinear controllers for such system is a challenging task. These systems are based on magnetic repulsion and attraction principle. In recent studies many researchers proposed controllers using various linear and nonlinear control techniques. Linear controllers are suitable when the system model is linearized in a small region while they do not cater for the nonlinearities present in the actual model of the system. Nonlinear controllers on the other hand provide a real time control for the system by controlling its dynamics globally instead of locally. The quest to propose an effective topology for designing perfect nonlinear controller would never end and the best one will fulfill the desired performance criterion in a suitable and promising manner. The basic criterion for selecting the nonlinear controller is to see the one which gives fast and efficient dynamic response i.e. lesser rise time, fast settling time, less peak value, minimum overshoot/undershoot and negligible steady state error. As real systems are prone to external disturbances, so the designed nonlinear controller should also be able to deal with these external disturbances smoothly and as efficiently as possible. Majority of the nonlinear controllers show poor or degraded performance in the presence of disturbances. Therefore, the basic motivation behind this research is to develop

The associate editor coordinating the review of this manuscript and approving it for publication was Ning Sun.

a robust nonlinear controller for controlling the MagLev system with best dynamic behavior and to cater for the effect of disturbances in an efficient way.

Motivation for this research has been gained by critically studying and evaluating different controllers presented in the literature for the control of MagLev systems. The problems associated with the existing controllers are analyzed and discussed in the following paragraphs and a potential solution to these problems is then proposed in the later sections of the paper.

Wiboonjaroen and Sujitjorn [13], presented a state-PID feedback based controller developed from the linearized version of the MagLev model to control the height of the ball. Real systems are nonlinear in nature and linearization of such systems results in compromising the efficiency and robustness of the controller. So keeping in view the demerits of linearized controllers, an active research has been started for designing better controllers which can cater the nonlinear nature of the systems without reducing them to linearized form. In [14], a nonlinear controller has been designed by using the feedback linearization technique for levitation of a metallic ball against the force of gravity using an electromagnet. The speed of the ball is not directly available; therefore nonlinear observer with linear error dynamics is designed. A linear feedback controller is also designed. Both of these controllers are then compared in terms of their dynamic performance to step inputs. However the main limitation of this scheme is concerned with the operating point of a system. If the operating point of a system is the same at which the model is linearized then a better response would be obtained. On the other hand if the operating point is far away from the point at which the system is linearized, then the tracking error would become large and dynamic performance would become worst. Likewise in [15], a nonlinear recursive controller is designed using state transformation and Lyapunov's direct method for assuring the global stability of MagLev system. The method uses the nonlinear model of the system and performs well when compared to linear controllers but there are certain overshoots/undershoots present in the response which is not desirable.

A lot of research based upon fuzzy logic controller (FLC) and artificial neural networking (ANN) has been done for the control of MagLev systems. FLC based controllers do not require any mathematical model of the system and thus depend completely upon human reasoning. In fuzzy logic, membership functions are used for each variable to be controlled where membership values are assigned in the range from 0 to 1. The input and output values are mapped according to designer's wish and is done using if-else statement based rules. The major disadvantage of FLC based algorithm is the non-availability of exact information about the system which renders the designed controller a primitive one. In [16] an adaptive fuzzy controller is designed for controlling the suspension system of medium-low-speed MagLev train by utilizing the data obtained by the application of internet of things (IoT). The adaptive fuzzy scheme is fast and feasible but only depends upon the available data and the rules to be made according to the situation. It does not utilize the actual nonlinear model of the system for designing the controller. Also the results show a lot of oscillations around the desired air gap value and a delayed convergence rate. Similarly, ANN based controllers also do not require systems' mathematical model but they do require training data for updating the weights of the neurons. Most of the time neural networks are used for tuning fuzzy parameters in order to introduce adaptability. Y. K. Teklehaimanot *et al.* in [17] uses a hybrid neuro-fuzzy controller to keep the train suspended in the air in the desired position in presence of uncertainties. The training data is generated by using PID controller. The results show good dynamic behavior but still the performance is dependent upon the training data and the rules used in fuzzy controller. Also there is a delay in convergence in the presence of disturbances.

The FLC and ANN based techniques can also be used along with nonlinear techniques in order to have a real time control by utilizing the nonlinear model of the system. In [3] an adaptive neural-fuzzy sliding mode controller is proposed for disturbance rejection and parameter perturbations in MagLev train system. The proposed controller shows satisfactory results but with some delays and chattering. Similarly in [18] an adaptive sliding mode control with RBF neural network estimator is implemented to control the MagLev system. The results show good performance in tracking of air gap but when constant disturbance is added it shows large overshoots and undershoots and also the delayed convergence to its reference value.

Recently some nonlinear controllers have been implemented in [19] for controlling MagLev system. Synergetic controller is designed which is able to control the system but not as efficiently as other nonlinear controllers due to delayed convergence and relatively larger steady state error. Backstepping (BS) is a recursive technique which uses Lyapunov theory for designing a controller for the overall system ensuring the global asymptotic stability [20]. For implementing backstepping technique, the system has to be in strict feedback form and is thus divided into different chunks. The control law is derived for each chunk and thus at the end a cumulative control law for the overall system is derived. The stability of the system should be ensured at each chunk so that the overall system is stable at the final stage. It is a systematic approach for designing a controller. It does not reduce the order of the system thus increasing the complexity to design a controller. As in [19] BS has relatively larger steady state error which can be further reduced by adding an integrator term in backstepping controller. Integral backstepping (IBS) reduces the steady state error but does not eliminate it. The rise time and settling time of the IBS can further be reduced by reducing the computational burden i.e. by reducing the order of the system and by designing a sliding surface as in the case of sliding mode control.

All the reviewed controllers have their own merits and demerits but most of them have delayed convergence,

chattering and undesired overshoots/undershoots during tracking of desired trajectories.

Now after having a comprehensive literature review on the methods proposed for controlling MagLev system, there are some points which are to be addressed for designing a better controller for these systems. The basic requirement is the enhancement in dynamic response of the system so that the proposed controller should have characteristics like: minimal overshoot/undershoot, faster convergence rate, minimal or zero steady state error and reduced chattering and robustness against external disturbance. For addressing all these requirements we choose supertwisting algorithm for designing our proposed controller.

Supertwisting is a higher order sliding mode controller which has the property to reduce chattering [21] which is an undesirable phenomenon in many systems. The dynamic response is very much enhanced as shown by results in this paper. Moreover, it is robust against disturbances and noises. It is computationally less costly because it does not require the derivative of the sliding surface as compared to conventional sliding mode control. In MagLev system the metallic object (ball) has to be levitated exactly at the desired air gap in a finite time by tracking the magnetic flux at the reference value. Also the momentum of the ball should remain zero and should quickly converge to zero in the presence of disturbances. Therefore, selecting supertwisting for designing a nonlinear controller is one of the most suitable options as compared to others. Therefore the main contribution of this research is the designing of a nonlinear robust controller using supertwisting which can enhance the dynamic performance, can reduce chattering and make the system robust against external disturbances and noises.

The paper proposed another robust controller based on integral backstepping sliding mode technique. The purpose of designing the second controller is to compare the robustness of the ST-SMC with that of IBS-SMC. The proposed controller is also compared with the controllers proposed in [26] and the comparison leads to the conclusion that among all the compared nonlinear controllers, ST-SMC shows the best performance so far.

The rest of the paper is arranged in the following pattern: Section II contains the basic principle of MagLev systems where the circuitry is explained with key parameters. Mathematical modeling is discussed in section III. The controller design is explained in section IV, where both the ST-SMC and IBS-SMC based controllers along with their stability proofs are discussed in subsections III-A and III-B respectively. Further, in section IV simulation results along with detailed comparative analysis is presented. Section V concludes the paper.

II. WORKING PRINCIPLE

MagLev system as shown in Fig.1 is composed of following two main parts:

- Electrical part
- Mechanical part

Electrical part consists of solenoid and a DC power source. The current i passes through the coil wrapped around the iron core. This arrangement will produce a magnetic field for aligning all the atoms. The potential difference produced by direct current source is used to give electrical signal in the form of electrical current to the coil. Electrical signal is converted into mechanical action with the help of the coil. In mechanical part, the distance of the iron ball from the center of solenoid can be adjusted by the voltage 'U' of DC source. The varying sequence of mechanical control starts by adjusting the DC voltage which in turn changes the amount of current i in the coil. So, the amount of flux λ passing through it also changes, which affects the magnetic force F_m acting on the iron ball.

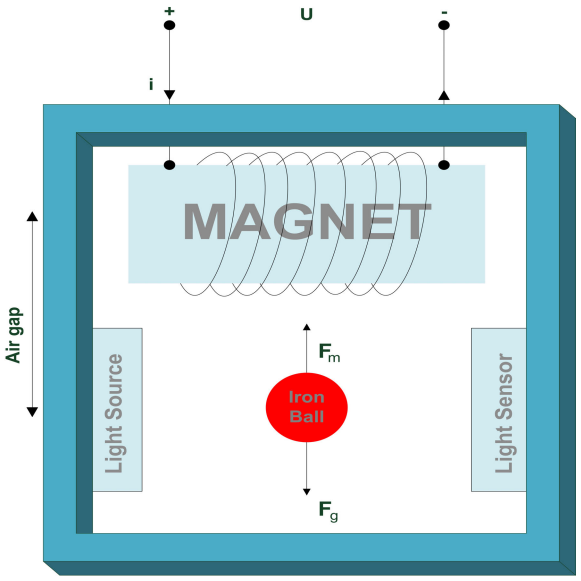

FIGURE 1. Circuit diagram of MagLev system.

It is evident from Fig.1 that there are two forces acting on the ball at a time; one is the magnetic force F_m produced due to flux linkage and the other is the gravitational force F_g acting in the opposite direction (downwards). The net force F_{net} on the ball can be written as:

$$F_{net} = F_m - F_g \tag{1}$$

The air gap is inversely proportional to the magnetic force on the ball i.e. with the increase in magnetic field, the air gap between the center of solenoid and the ball is decreased. In levitated position we can write:

$$F_{net} = 0 \tag{2}$$

III. MATHEMATICAL MODELLING

To explain the dynamical behavior of the system using its mechanical and electrical components, consider an iron ball present in the vicinity of magnetic field produced by a single magnet. The equations for this system as described

in [22], [23] and [19] are given as:

$$\dot{\lambda} + Ri = u \tag{3}$$

$$m\ddot{\theta} = F_{\text{m-mg}} \tag{4}$$

Eq. (3) is derived by invoking Kirchhoff's voltage law while Eq. (4) is derived using Newton's second law, where:

- λ is the flux produced by the field and depends upon θ and is given by:

$$\lambda = L(\theta)i \tag{5}$$

- θ is the air gap between the center of the iron ball and magnetic coil
- g is the gravitational constant (9.81 m/s^2)
- R is the resistance
- F_m is the magnetic force given as:

The magnetic force F_m is given as:

$$F_m = \frac{1}{2}\frac{\partial L(\theta)}{\partial \theta} i^2 \tag{6}$$

Now an approximation to L (inductance) of coil can be given by the formula:

$$L = \frac{k}{1-\theta} \tag{7}$$

where domain of L is restricted to $-\infty < \theta < 1$ i.e: normalizing the nominal gap to 1, while k which is a positive number, depends upon the number of coil turns. Using the value of L in Eq. (5), we get the current i as:

$$i = \frac{(1-\theta)\lambda}{k} \tag{8}$$

Updating Eq. (3) by using the value of i from Eq. (8), we have:

$$\dot{\lambda} + \frac{R(1-\theta)\lambda}{k} = u \tag{9}$$

Substituting the value of F_m in Eq. (4), we get:

$$m\ddot{\theta} = \frac{1}{2}\frac{\partial L(\theta)}{\partial \theta} i^2 - mg \tag{10}$$

The momentum of the ball in terms of mass and velocity is:

$$\rho = m\dot{\theta} \tag{11}$$

which gives:

$$\dot{\theta} = \frac{\rho}{m} \tag{12}$$

Time derivative of Eq. (11) gives:

$$m\ddot{\theta} = \dot{\rho} \tag{13}$$

substituting $m\ddot{\theta}$ in Eq. (10), we get:

$$\dot{\rho} = \frac{1}{2}\frac{\partial L(\theta)}{\partial \theta} i^2 - mg \tag{14}$$

Now $\frac{\partial L(\theta)}{\partial \theta}$ can be found by using Eq. (7) as:

$$\frac{\partial L(\theta)}{\partial \theta} = \frac{k}{(1-\theta)^2} \tag{15}$$

Using Eq. (15), the updated $\dot{\rho}$ can be obtained by using Eq. (14) yields:

$$\dot{\rho} = \frac{\lambda^2}{2k} - mg \tag{16}$$

Therefore, from equations (9), (12) and (16), the generalized model of considered system is represented as:

$$\dot{\lambda} + \frac{R(1-\theta)\lambda}{k} = u \tag{17}$$

$$\dot{\theta} = \frac{\rho}{m} \tag{18}$$

$$\dot{\rho} = \frac{\lambda^2}{2k} - mg \tag{19}$$

Now by defining state system as $x = [x_1\ x_2\ x_3]^T = [\theta\ \rho\ \lambda]^T$, we get the compact form of the system of Eqs. (17)-(19) which is suitable for controller design as:

$$\dot{x}_1 = \frac{x_2}{m} \tag{20}$$

$$\dot{x}_2 = \frac{x_3^2}{2k} - mg \tag{21}$$

$$\dot{x}_3 = -\frac{R(1-x_1)x_3}{k} + u \tag{22}$$

IV. CONTROLLER DESIGN

Equations (20-22) represent the magnetic levitation system where the presence of x_3^2 term and product term x_1x_3 makes the system nonlinear. So to efficiently control this system and to achieve the desired control objectives, an effective and robust nonlinear controller is required. Fig.(2) shows the general block diagram of the feedback system where error between desired and actual position of the iron ball is used in feedback path for the control purpose.

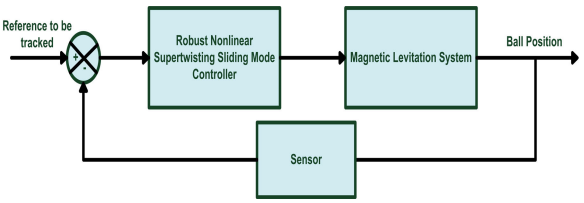

FIGURE 2. Flow diagram of control of MagLev system.

The controllers are to be designed in such a way that fulfill the following objectives may be fulfilled:

- Maintaining the desired air gap
- Tracking of desired magnetic flux which is required for maintaining the air gap
- Convergence of the momentum of the ball to zero
- Global asymptotic stability of the overall system.

A. SUPER TWISTING SLIDING MODE CONTROL

For designing the supertwisting based SMC control algorithm, we first have to select a sliding surface. A number of methods are available for designing of different kind of sliding surfaces out of which the error based surface design is the simplest one. So we select this method for better tracking

of the desired values of all the states of the system. Now the difference between actual and desired values is considered as errors given by:

$$e_1 = x_1 - x_{1ref} \tag{23}$$
$$e_2 = x_2 - x_{2ref} \tag{24}$$
$$e_3 = x_3 - x_{3ref} \tag{25}$$

where, x_{1ref}, x_{2ref} and x_{3ref} are the reference values for desired air gap, momentum and flux respectively.

The sliding surface σ for our controller is taken as

$$\sigma = c_1 e_1 + c_2 e_2 + c_3 e_3 \tag{26}$$

Derivative of Eq. (26) with respect to time yields:

$$\dot{\sigma} = c_1 \dot{e}_1 + c_2 \dot{e}_2 + c_3 \dot{e}_3 \tag{27}$$

Similarly, taking time derivatives of equations (23)-(25), we have:

$$\dot{e}_1 = \dot{x}_1 - \dot{x}_{1ref} \tag{28}$$
$$\dot{e}_2 = \dot{x}_2 - \dot{x}_{2ref} \tag{29}$$
$$\dot{e}_3 = \dot{x}_3 - \dot{x}_{3ref} \tag{30}$$

Putting the values of $\dot{e}_1$, $\dot{e}_2$ and $\dot{e}_3$ in Eq. (27), we get:

$$\dot{\sigma} = c_1(\dot{x}_1 - \dot{x}_{1ref}) + c_2(\dot{x}_2 - \dot{x}_{2ref}) + c_3(\dot{x}_3 - \dot{x}_{3ref}) \tag{31}$$

Substituting $\dot{x}_3$ from Eq. (22) and putting $\dot{\sigma} = 0$ in Eq. (33), we get the equivalent controller u_{equ} as:

$$u_{equ} = -\frac{1}{c_3}[c_1(\dot{x}_1 - \dot{x}_{1ref}) + c_2(\dot{x}_2 - \dot{x}_{1ref}) + c_3\dot{x}_{3ref} - \frac{c_3 R(1-x_1)y_3}{k}] \tag{32}$$

Next, the switching control for supertwisting sliding mode u_{sw} can be written as:

$$\begin{cases} u_{sw} = -k_1|\sigma|^{(0.5)}sign(\sigma) + u_1 \\ \dot{u}_1 = -k_2 sign(\sigma) \end{cases} \tag{33}$$

or

$$u_{sw} = -k_1|\sigma|^{(0.5)}sign(\sigma) - k_2\int sign(\sigma)d(\tau) \tag{34}$$

where k_1 and k_2 are given [24] as:

$$k_2 > \frac{\psi}{\Gamma_{min}} \tag{35}$$
$$k_1^2 \geq \frac{4\psi\Gamma_{max}(k_2+\psi)}{\Gamma_{min}^2\Gamma_{min}(k_2-\psi)} \tag{36}$$

with conditions

$$\psi > |\frac{d\dot{\sigma}}{dt} + \frac{d\dot{\sigma}}{dx}[f(x,t) + b(t)u(t) + d(t)]| \tag{37}$$

and

$$0 \leq \Gamma_{min} \leq |\frac{d\dot{\sigma}}{du}| \leq \Gamma_{max} \tag{38}$$

The overall control law for ST-SMC can be written as:

$$u_{ST-SMC} = u_{equ} + u_{sw} \tag{39}$$

To study the stability of the proposed controller [25], [26], following conditions should be fulfilled:

- V is positive definite
- V is radially unbounded
- $\dot{V}$ is negative definite

Taking Lyapunov candidate function as:

$$V = \frac{1}{2}\sigma^2 \tag{40}$$

From Eq. (40), the first two conditions are satisfied. Derivative of Eq. (40) with respect to time yields:

$$\dot{V} = \sigma\dot{\sigma} \tag{41}$$

Substituting $\dot{\sigma}$ from Eq. (27) in Eq. (41), we have:

$$\dot{V} = \sigma(c_1\dot{e}_1 + c_2\dot{e}_2 + c_3\dot{e}_3) \tag{42}$$

Now, substituting $\dot{x}_3$ from Eq. (22) in Eq. (42) gives:

$$\dot{V} = \sigma\left(c_1\dot{e}_1 + c_2\dot{e}_2 + c_3\left(-\frac{R(1-x_1)x_3}{k} + u\right)\right) \tag{43}$$

Finally, by substituting u from Eq. (34) in Eq. (41), we get:

$$\dot{V} = \sigma\left(-k_1|s|^{0.5}sign(\sigma) - k_2\int sign(\sigma)d(\tau)\right) \tag{44}$$

Simplification of Eq. (44) yields:

$$\dot{V} = -k_1|\sigma|^{0.5}|\sigma| - k_2\int|\sigma|d(\tau) \tag{45}$$

Eq. (45) shows that $\dot{V}$ is negative definite which means that the asymptotic stability of controller is ensured where parameters (k_1 and k_2) are chosen in accordance with conditions given by equations (34) and (35).

B. INTEGRAL BACKSTEPPING SLIDING MODE CONTROL

In this section a nonlinear controller based on integral backstepping sliding mode technique is designed. For this purpose we will derive an equivalent control by using integral backstepping technique and then we will incorporate switching control to complete the design of our controller. For this purpose we take the error between the actual and desired values of the state x_2 i.e: momentum of the iron ball.

$$e_{11} = x_2 - x_{2ref} \tag{46}$$

Time derivative of the Eq. (46) results in:

$$\dot{e}_{11} = \dot{x}_2 - \dot{x}_{2ref} \tag{47}$$

Substituting $\dot{x}_2$ from Eq. (21) in Eq. (47), we have:

$$\dot{e}_{11} = \frac{x_3^2}{2k} - mg - \dot{x}_{2ref} \tag{48}$$

For incorporating integral action in backstepping, introduce the integrator term as:

$$\phi = \int_0^t (x_2 - x_{2ref})dt \tag{49}$$

Taking time derivative of Eq. (49) gives:

$$\dot{\phi} = x_2 - x_{2ref} \tag{50}$$

From Eq. (50), it is clear that:

$$\dot{\phi} = e_{11} \tag{51}$$

Next, a Lyapunov candidate function can be taken as:

$$V_1 = \frac{1}{2}e_{11}^2 + \frac{\gamma}{2}\phi^2 \tag{52}$$

Time derivative of Eq. (50) yields:

$$\dot{V}_1 = e_{11}\dot{e}_{11} + \gamma\phi e_{11} \tag{53}$$

By substituting $\dot{e}_{11}$ from Eq. (48) in Eq. (51), we have:

$$\dot{V}_1 = e_{11}\left(\frac{x_3^2}{2k} - mg - \dot{x}_{2ref} + \gamma\phi\right) \tag{54}$$

Now for the stability of the system, we can take:

$$\frac{x_3^2}{2k} - mg - \dot{x}_{2ref} + \gamma\phi = -c_1 e_{11} \tag{55}$$

where c_1 is a positive number. Eq. (54) thus becomes:

$$\dot{V}_1 = -c_1 e_{11}^2 \tag{56}$$

Eq. (56) shows that $\dot{V}$ is negative definite. Now considering x_3 as a virtual control law which will serve as a reference for the next state, Eq. (55) gives:

$$x_3 = (-2kc_1e_{11} + 2kmg + 2k\dot{x}_{2ref} - 2k\gamma\phi)^{\frac{1}{2}} \tag{57}$$

Taking $x_3 = \nu$ and defining the next error as:

$$e_{22} = x_3 - \nu \tag{58}$$

Time derivative of Eq. (58) yields:

$$\dot{e}_{22} = \dot{x}_3 - \dot{\nu} \tag{59}$$

Now for $\dot{\nu}$, time derivative of Eq. (57) results in:

$$\dot{\nu} = (-2kc_1e_{11} + 2kmg + 2k\dot{x}_{2ref} - 2k\gamma\phi)^{-\frac{1}{2}} \times (-2kc_1\dot{e}_{11} + 2k\ddot{x}_{2ref} - 2k\gamma e_{11}) \tag{60}$$

For simplicity take

$$\dot{\nu} = \frac{1}{2}G(e_{11}) \tag{61}$$

where $G(e_{11})$ is a function of e_{11}. The cumulative Lyapunov candidate function is taken as:

$$V_c = V_1 + \frac{1}{2}e_{22}^2 \tag{62}$$

Updating $\dot{e}_{11}$ using Eq. (48), we have:

$$\dot{e}_{11} = \frac{(e_{22} + \nu)^2}{2k} - mg - \dot{x}_{2ref} \tag{63}$$

The Eq. (57) gives:

$$\nu^2 = -2kc_1e_{11} + 2kmg + 2k\dot{x}_{2ref} - 2k\gamma\phi \tag{64}$$

Putting ν^2 from Eq. (64) in Eq. (63), results in:

$$\dot{e}_{11} = \frac{e_{22}^2}{2k} - c_1e_{11} - \gamma\phi + \frac{e_{22}\nu}{k} \tag{65}$$

Time derivative of Eq. (62) is:

$$\dot{V}_c = \dot{V}_1 + e_{22}\dot{e}_{22} \tag{66}$$

Using $\dot{V}_1$ from Eq. (54), we have:

$$\dot{V}_c = -c_1e_{11}^2 + e_{22}\left(\frac{e_{11}e_{22}}{2k} + \frac{e_{11}\nu}{k} + \dot{e}_{22}\right) \tag{67}$$

Now by taking:

$$\frac{e_{11}e_{22}}{2k} + \frac{e_{11}\nu}{k} + \dot{e}_{22} = -c_2e_{22} \tag{68}$$

the stability of the system is ensured as:

$$\dot{V}_c = -c_1e_{11}^2 - c_2e_{22}^2 \tag{69}$$

Now from Eq. (68), we can get $\dot{e}_2$ as:

$$\dot{e}_{22} = -c_2e_{22} - \frac{e_{11}e_{22}}{2k} - \frac{e_{11}\nu}{k} \tag{70}$$

Putting the values of $\dot{e}_{22}$, $\dot{x}_3$, and $\dot{\nu}$ from Eq. (70), Eq. (22) and Eq. (60) respectively in Eq. (59), we get:

$$-c_2e_{22} - \frac{e_{11}e_{22}}{2k} - \frac{e_{11}\nu}{k} = -\frac{R(1-x_1)x_3}{k} + u - \frac{1}{2}G(e_{11}) \tag{71}$$

Hence by using Eq. (69), our equivalent control u_{equ} comes out to be:

$$u_{equ} = \frac{R(1-x_1)x_3}{k} + \frac{1}{2}G(e_{11}) - c_2e_{22} - \frac{e_{11}e_{22}}{2k} - \frac{e_{11}\alpha}{k} \tag{72}$$

Now, incorporating the sliding mode control in integral backstepping for making the controller robust, we have to add the switching control given as:

$$u_{sw} = -k_1 sign(\sigma) \tag{73}$$

Therefore the overall control thus becomes:

$$u = u_{equ} + u_{sw} \tag{74}$$

Using Eq. (72) and Eq. (73), we have:

$$u = \frac{R(1-x_1)x_3}{k} + \frac{1}{2}G(e_{11}) - c_2e_{22} - \frac{e_{11}e_{22}}{2k} - \frac{e_{11}\alpha}{k} - k_1 sign(\sigma) \tag{75}$$

which represents the desired nonlinear control law.

C. BACKSTEPPING SLIDING MODE CONTROL

By eliminating the integral term, an expression for backstepping sliding mode control can be obtained as follows.

$$u = \frac{R(1-x_1)x_3}{k} + \frac{1}{2}B(e_{11}) - c_2 e_{22} - \frac{e_{11}e_{22}}{2k} - \frac{e_{11}\alpha}{k} - k_1 sign(\sigma) \quad (76)$$

where

$$\frac{1}{2}B(e_{11}) = (-2kc_1 e_{11} + 2\,kmg + 2k\dot{x}_{2ref})^{\frac{-1}{2}} \times (-2kc_1\dot{e}_{11} + 2k\ddot{x}_{2ref} - 2k\gamma e_{11}) \quad (77)$$

The simulation results of these proposed controllers are given in next section.

V. SIMULATIONS AND RESULTS

The validity of the proposed controllers can be analyzed by simulating their outputs in MATLAB/Simulink environment. The circuit components along with their values are presented in Table 1. The values are selected same as in [**?**], in order to establish a comparison between the proposed nonlinear controllers and the existing ones.

TABLE 1. Circuit components and values.

Parameters	Values
Coil Inductance (L)	0.01 H
Resistance (R)	1 Ω
Mass of iron ball (m)	1 g
Coil constant (k)	1
Gravitational constant (g)	9.8 m/s^2

The values of gains for ST-SMC are calculated such that they satisfy the bounds given by equations (36) and (37), whereas the values for the gain parameters for IBS-SMC are chosen on hit and trial basis (values are changed if the response of the system is not what is desired). The gain values can also be found optimally or by using complex techniques like neural networks at the cost of calculation complexity. Table 2 lists the gain values for both the proposed controllers.

The air-gap reference is set at 2 cm which is to be tracked by the state x_1. The response of air-gap is started from time t = 0 and the initial condition for the air-gap is taken as $x_1(0)$=1.895 cm.

Fig.3 corresponds to the comparative analysis of air-gap tracking response of all the proposed nonlinear controllers. For the case of IBS-SMC rise time for the waveform comes out to be 0.2238 s and the settling time for IBS-SMC is 0.3540s. There is no undershoot present while a very small overshoot of 0.0714 is observed. The peak time for this response is 0.635 s which corresponds to the peak value of 2.0014. Steady state error for IBS-SMC 0.0014 is negligibly small. Moreover chattering phenomenon due to the presence of switching control in IBS-SMC can be observed in the steady state response of IBS-SMC. In case of ST-SMC it

TABLE 2. Parametric values of the controllers.

Controller	parameters	Values
Super twisting sliding mode control	k_1	1
	k_2	50
Integral backstepping sliding mode control	c_1	9
	c_2	43.8
	γ	0.0012
Backstepping control [20]	c_1	2
	c_2	10.62
Integral Backstepping control [20]	c_1	7.865
	c_2	3.92
	β	0.003
Synergetic control [20]	w_0	6
	w_1	3.03
	w_2	0.99
	T	0.99

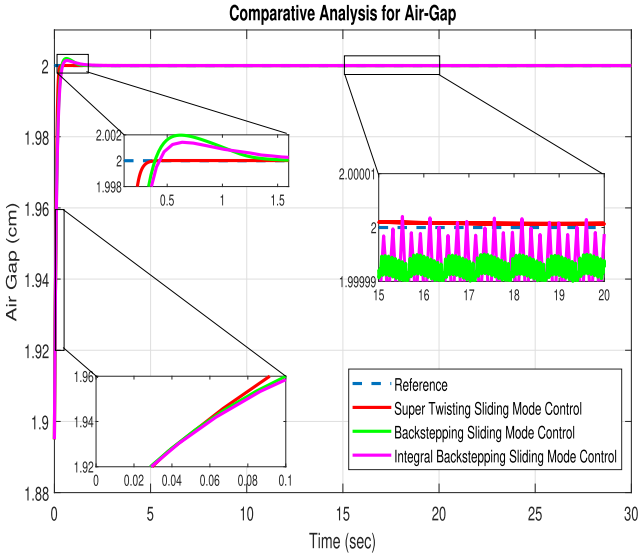

FIGURE 3. Comparative analysis for Air-Gap.

can be seen that there is no undershoot and overshoot present. The rise time is 0.1531s and the settling time is 0.2279 s, the peak time of 0.6678 s corresponds to the peak value of 2.000, zero steady state error and no chattering present in the state response. Therefore by comparison it can be seen that steady state error is maximum in case of BS-SMC. Addition of an integral term in case of IBS-SMC results in the reduction of steady state error whereas the ST-SMC depicts almost zero steady state error and almost zero chattering while IBS-SMC has less chattering and steady state error as compared to BS-SMC. Furthermore ST-SMC has the faster convergence as compared to IBS-SMC and BS-SMC.

The momentum of the iron ball should be zero in the presence of magnetic field. Figure 4 represents the comparative analysis of momentum tracking by all the proposed controllers. In case of IBS-SMC, settling time is 0.4250 s

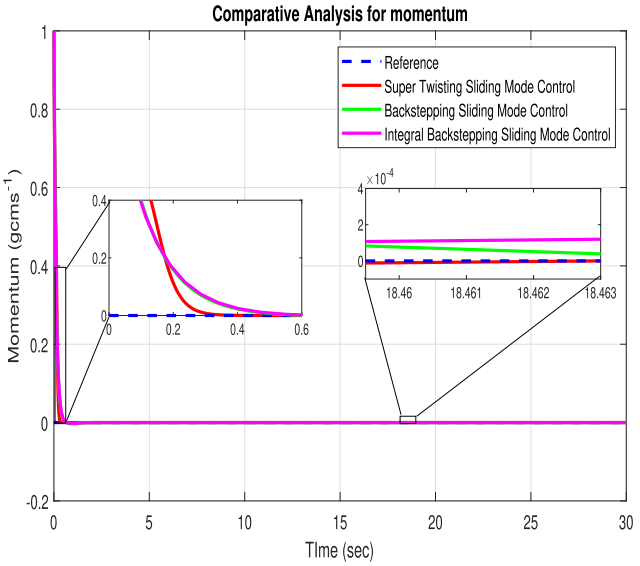

FIGURE 4. Comparative analysis for momentum.

but there is still delayed convergence and steady state error is present. In ST-SMC case, settling time is 0.2669 s and there is reduction in convergence time which is present in case of IBS-SMC. Further, zero steady state error shows perfect tracking of momentum to its reference value. The responses of both IBS-SMC and BS-SMC are almost same initially, however, they differ minutely afterwards. Moreover the steady state error and convergence of ST-SMC are greatly improved which highlights the clear dominance of super twisting algorithm when compared with both IBS-SMC and BS-SMC.

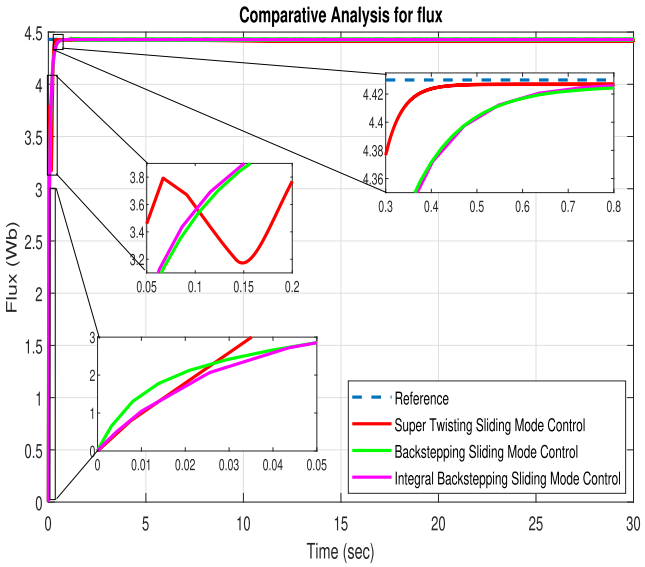

FIGURE 5. Comparative analysis for flux.

Comparison of all the nonlinear controllers for tracking the desired flux has been presented in Fig.5. The settling time for IBS-SMC and BS-SMC are 0.3558s and 0.3519s respectively with no undershoot and overshoot. Both IBS-SMC and BS-SMC show smooth response, yet they have delayed convergence and more steady state error. ST-SMC algorithm being fast enough shows some transients at the beginning but have faster convergence than other controllers. Furthermore, ST-SMC has zero steady state error while tracking the desired flux.

Now for the purpose of checking the behavior of proposed controllers under the effect of noise, a Gaussian type noise with $\mu = 0, \sigma = 9.8969 \times 10^{-6}$ and $t = 0.0044\ s$ is added to the system as shown in Fig.6.

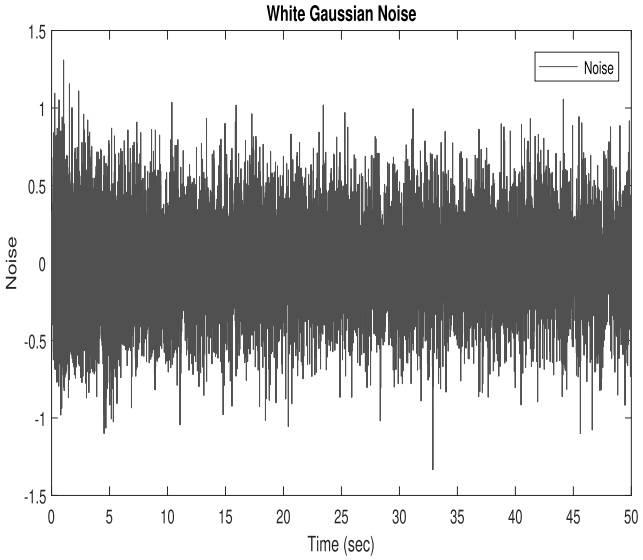

FIGURE 6. Gaussain noise.

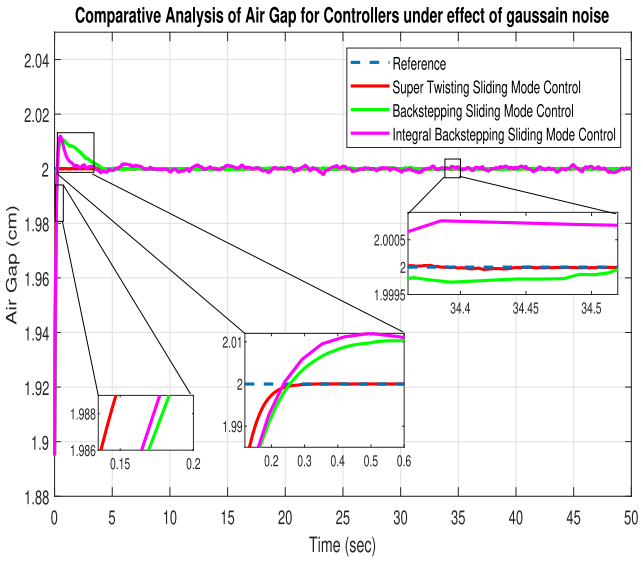

FIGURE 7. Comparative analysis for Air-Gap under the effect of noise.

The response of the air-gap of the system under the effect of Gaussian noise is shown in the Fig.7. The response of nonlinear controllers is very fast and tracking is preserved when

TABLE 3. Comparison of all the controllers.

Response	PI	Synergetic	BS	IBS	BS-SMC	IBS-SMC	ST-SMC
Rise Time(s)	0.1053	0.2082	0.1954	0.1756	0.2137	0.2238	0.1531
Settling Time(s)	15.9026	0.3477	0.2863	0.2587	0.3292	0.3540	0.2279
Overshoot (cm)	0.3736	0	0	0	0.0987	0.0714	0
Undershoot (cm)	0.16	0	0	0	0	0	0
Peak Time (s)	0.9294	0.5980	0.3893	0.3342	0.6326	0.6357	0.6678
Peak Value (cm)	2.3736	2.0003	2.0002	2.00001	2.0020	2.0014	2.0000
Steady State Error	0.0001	0.0003	0.0002	0.00001	0.002	0.0014	0

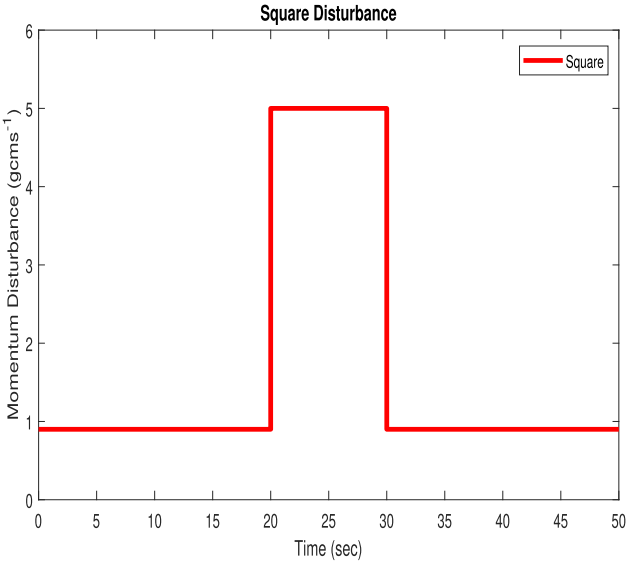

FIGURE 8. Square disturbance.

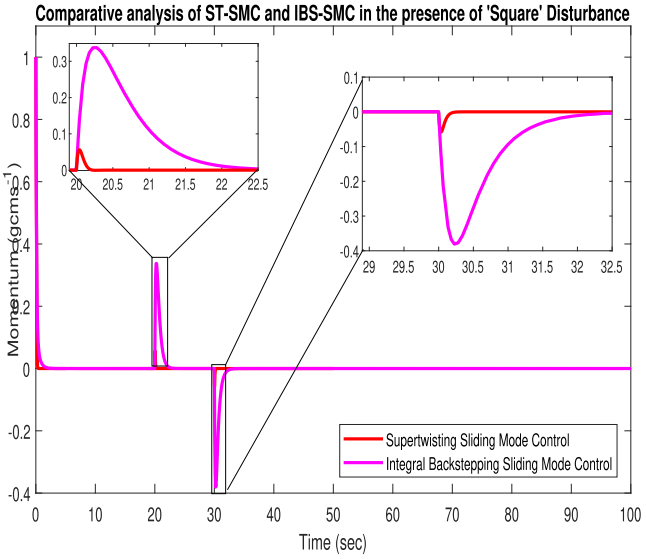

FIGURE 10. Momentum under the effect of disturbance.

compared with linear PI controllers. Relatively larger overshoots are observed in case of both IBS-SMC and BS-SMC while there is no overshoot/undershoot present in case of ST-SMC. Also both IBS-SMC and BS-SMC have larger steady state error as compared to ST-SMC.

For assessing the robustness of ST-SMC and IBS-SMC, a square type disturbance is added in the momentum state of the system as shown in the Fig.8. while the closed loop system with added disturbance is shown in Fig.9.

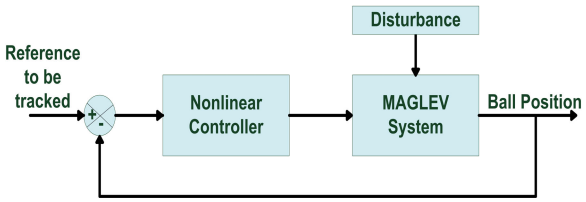

FIGURE 9. Flow diagram with added disturbance.

The response of momentum state under the effect of external disturbance is shown in Fig.10. It can be seen that at the time instant when disturbance occurs both the controllers reject the effect of disturbance and track the reference nicely. There are overshoots/undershoots at the beginning and at the end of the disturbance. It can be observed that the peak of shoot in case of IBS-SMC is larger than that of ST-SMC. Although both are robust in nature, yet ST-SMC performs better than IBS-SMC as it shows less overshoots and fast convergence to reference value in the presence of external disturbances.

VI. COMPARISON BETWEEN CONTROL TECHNIQUES

For the comparison of different aspects of few existing in the literature and proposed nonlinear controllers, Table 3 has been formulated in order to highlight their pros and cons. The dynamic response values of the existing controllers are obtained from [19].

The linear PI controller has a rise time of 0.1053s which is lowest among all the other controllers. The major disadvantage of PI controller is the settling time of 15.9026s which

is very high when compared with all the proposed nonlinear controllers. The rise time of ST-SMC do not vary much as in case of PI but in terms of settling time PI shows the slowest while ST-SMC shows the fastest convergence rate. Further, ST-SMC also has considerable difference of peak value when compared to PI. This shows the superiority of ST-SMC over linear PI controllers.

Synergetic controller has a rise time of 0.2082 s and settling time of 0.3477s. These values are very large when compared to ST-SMC which show their slower convergence rate. It also has a steady state error of 0.0003 whereas ST-SMC has a zero steady state error. Thus ST-SMC outperforms synergetic controller in every aspect. BS and IBS have rise time of 0.1954s and 0.1756s respectively. Although both these controllers show small rise time, yet the rise time of ST-SMC is smaller. The comparison of settling time of both BS and IBS with ST-SMC shows fast convergence of ST-SMC. Furthermore, zero steady state error of ST-SMC shows the stable operation of the system whereas both BS and IBS have some steady state error present in them.

IBS-SMC has smaller overshoot as compared to BS-SMC and PI controller while it has zero undershoot when compared to linear PI controller. It also has less peak value when compared to BS-SMC and PI controller. IBS-SMC has a trade off with other nonlinear controllers as it has more settling time and rise time but it is robust against disturbances and noises. Although IBS-SMC is a robust controller but when compared with ST-SMC it shows delayed response as it has a settling time of 0.3292s compared to 0.2279s in case of ST-SMC. Also ST-SMC has no overshoot/undershoot while an overshoot of 0.0987 cm is present in IBS-SMC. The steady state error of IBS-SMC is also large as compared to ST-SMC. Hence when compared with IBS-SMC, ST-SMC shows better dynamic performance and enhanced robustness against disturbances.

Among all the nonlinear controllers, ST-SMC gives the best results. There is no undershoot and overshoot present and has the least rise time of 0.1531s when compared to other nonlinear controllers. In terms of settling time, it also outperforms all other compared controllers. No steady state error and least peak value of 2cm represent the perfect tracking of ST-SMC. Also, ST-SMC is robust against disturbances and noises and shows better results than that of IBS-SMC as shown in the simulations. In nutshell, ST-SMC has the best available features among other proposed nonlinear controllers.

VII. CONCLUSION

Maintaining the air gap of the levitated object, has been the main issue with MagLev systems. For this purpose, we proposed supertwisting SMC which not only removes the chattering but also is robust against external disturbances to the plant. The proposed integral backstepping SMC is not as efficient as supertwisting sliding node controller in terms of reducing. Comparison shows that ST-SMC gives the overall best dynamic response with negligible chattering and is robustness against external disturbances in controlling MagLev systems among all other compared nonlinear controllers. The future work includes the control of updated time varying dynamic model of MagLev system and the study of reducing the computational burden of ST-SMC in such particular applications.

REFERENCES

[1] T. Hu, Z. Lin, and P. E. Allaire, "Power-loss minimization in magnetic bearing systems," in *Proc. IEEE Conf. Decis. Control*, Jan. 2001, pp. 854–859.

[2] H.-W. Lee, K.-C. Kim, and J. Lee, "Review of maglev train technologies," *IEEE Trans. Magn.*, vol. 42, no. 7, pp. 1917–1925, Jul. 2006.

[3] Y. Sun, J. Xu, H. Qiang, and G. Lin, "Adaptive neural-fuzzy robust position control scheme for maglev train systems with experimental verification," *IEEE Trans. Ind. Electron.*, vol. 66, no. 11, pp. 8589–8599, Nov. 2019.

[4] J. Xu, Y. Sun, D. Gao, W. Ma, S. Luo, and Q. Qian, "Dynamic modeling and adaptive sliding mode control for a maglev train system based on a magnetic flux observer," *IEEE Access*, vol. 6, pp. 31571–31579, 2018.

[5] C. Chen, J. Xu, W. Ji, L. Rong, and G. Lin, "Sliding mode robust adaptive control of maglev Vehicle's nonlinear suspension system based on flexible track: Design and experiment," *IEEE Access*, vol. 7, pp. 41874–41884, 2019.

[6] T. Tezuka, N. Kurita, and T. Ishikawa, "Design and simulation of a five degrees of freedom active control magnetic levitated motor," *IEEE Trans. Magn.*, vol. 49, no. 5, pp. 2257–2262, May 2013.

[7] H. Wang and F. Li, "Levitation control of an improved modular bearingless switched reluctance motor," *ISA Trans.*, vol. 80, pp. 564–571, Sep. 2018.

[8] M. Osa, T. Masuzawa, R. Orihara, and E. Tatsumi, "Compact maglev motor with full DOF active control for miniaturized rotary blood pumps," in *Proc. 11th Int. Symp. Linear Drives Ind. Appl. (LDIA)*, Osaka, Japan, Sep. 2017, pp. 1–6.

[9] C. Kim, "Robust air-gap control of superconducting-hybrid MagLev intelligent conveyor system in smart factory," *IEEE Trans. Magn.*, vol. 55, no. 6, Jun. 2019, Art. no. 8300705.

[10] S. Verma, W. Kim, and H. Shakir, "Multi-axis maglev nanopositioner for precision manufacturing and manipulation applications," *IEEE Trans. Ind. Appl.*, vol. 41, no. 5, pp. 1159–1167, Sep. 2005.

[11] R. Cao, Y. Jin, M. Lu, and Z. Zhang, "Quantitative comparison of linear flux-switching permanent magnet motor with linear induction motor for electromagnetic launch system," *IEEE Trans. Ind. Electron.*, vol. 65, no. 9, pp. 7569–7578, Sep. 2018.

[12] J. R. Hull, J. Fiske, K. Ricci, and M. Ricci, "Analysis of levitational systems for a superconducting launch ring," *IEEE Trans. Appl. Supercond.*, vol. 17, no. 2, pp. 2117–2120, Jun. 2007.

[13] W. Wiboonjaroen and S. Sujitjorn, "State-PID feedback for magnetic levitation system," *Advanced Materials Research*, vols. 622–623, pp. 1467–1473, Dec. 2012.

[14] W. Barie and J. Chiasson, "Linear and nonlinear state-space controllers for magnetic levitation," International Journal of Systems Science, vol. 27, no. 11, pp. 1153–1163, 1996.

[15] J. Kaloust, C. Ham, J. Siehling, E. Jongekryg, and Q. Han, "Nonlinear robust control design for levitation and propulsion of a maglev system," *IEE Proc. Control Theory Appl.*, vol. 151, no. 4, pp. 460–464, Jul. 2004.

[16] Y. Sun, H. Qiang, J. Xu, and G. Lin, "Internet of Things-based online condition monitor and improved adaptive fuzzy control for a medium-low-speed maglev train system," *IEEE Trans Ind. Informat.*, vol. 16, no. 4, pp. 2629–2639, Apr. 2020.

[17] Y. K. Teklehaimanot, D. S. Negash, E. A. Workiye, "Design of hybrid neuro-fuzzy controller for magnetic levitation train systems," in *Information and Communication Technology for Development for Africa* (Communications in Computer and Information Science), vol. 1026, F. Mekuria, E. Nigussie, and T. Tegegne, Eds. Cham, Switzerland: Springer, 2019.

[18] Y. Sun, J. Xu, H. Qiang, C. Chen, and G. Lin, "Adaptive sliding mode control of MagLev system based on RBF neural network minimum parameter learning method," *Measurement*, vol. 141, pp. 217–226, Jul. 2019.

[19] A. S. Malik, I. Ahmad, A. U. Rahman, and Y. Islam, "Integral backstepping and synergetic control of magnetic levitation system," *IEEE Access*, vol. 7, pp. 173230–173239, 2019.

[20] H. K. Khalil, *Nonlinear Systems*, 3rd ed. Upper Saddle River, NJ, USA: Prentice-Hall, 2002.

[21] A. Swikir and V. Utkin, "Chattering analysis of conventional and super twisting sliding mode control algorithm," in *Proc. 14th Int. Workshop Variable Struct. Syst. (VSS)*, Jun. 2016, pp. 98–102.
[22] L. Qi, J. Cai, A. Han, J. Wan, C. Mei, and Y. Luo, "A novel nonlinear control technique with its application to magnetic levitated systems," *IEEE Access*, vol. 6, pp. 78659–78665, 2018.
[23] R. Ortega, A. J. Van Der Schaft, I. Mareels, and B. Maschke, "Putting energy back in control," *IEEE Control Syst. Mag.*, vol. 21, no. 2, pp. 18–33, Apr. 2001.
[24] C. Kunusch, P. F. Puleston, M. A. Mayosky, and J. Riera, "Sliding mode strategy for PEM fuel cells stacks breathing control using a super-twisting algorithm," *IEEE Trans. Control Syst. Technol.*, vol. 17, no. 1, pp. 167–174, Jan. 2009.
[25] S. Ahmad, N. Ahmed, M. Ilyas, and W. Khan, "Super twisting sliding mode control algorithm for developing artificial pancreas in type 1 diabetes patients," *Biomedical Signal Processing and Control*, vol. 38, pp. 200–211, Sep. 2017.
[26] J. J. E. Slotine and W. Li, *Applied Nonlinear Control*, vol. 199. Upper Saddle River, NJ, USA: Prentice-Hall, 1991.

HAFIZ MIAN MUHAMMAD ADIL received the B.S. degree in electrical engineering from the University of Engineering and Technology, Lahore, in 2014. He is currently pursuing the M.S. degree in electrical engineering with specialization in power and control systems with the School of Electrical Engineering and Computer Science, National University of Sciences and Technology (NUST), Islamabad, Pakistan.

SHAHZAD AHMED received the B.S. degree in electrical engineering from the FAST-National University of Computer and Emerging Sciences, Islamabad, Pakistan, in 2017. He is currently pursuing the M.S. degree in electrical engineering with specialization in power and control systems with the School of Electrical Engineering and Computer Science, National University of Sciences and Technology (NUST), Islamabad.

IFTIKHAR AHMAD received the M.S. degree in fluid mechanical engineering from the University of Paris VI (University Pierre Marie Curie), Paris, and the Ph.D. degree in robotics, control and automation from the Universite de Versailles, France. He is currently an Assistant Professor with the Department of Electrical Engineering, School of Electrical Engineering and Computer Science, National University of Sciences and Technology (NUST), Islamabad, Pakistan. His main research interests include nonlinear systems, robotics, automation and control, hybrid electrical vehicles, and maximum power point tracking.